

A study on effect of transition on High Lift Configuration Aerodynamics

Wang Xun *, Jin Na *

*Science and Technology on Space Physics Laboratory, Beijing, 100076

Abstract

This research focuses on the effect of transition on aerodynamic characteristics of high lift configurations. To investigate transitional effect, numerical simulations are conducted on *multiple airfoils* *McDonald Douglas 30P30N* and *NASA Trapezoidal Wing*. The simulations are accomplished by an in-house code with γ - $Re_{\theta t}$ transition model. The calculated results are compared with experiments in NASA Langley low turbulent wind tunnel. Test cases are run with and without transitional modeling. The results show that using fully turbulent model (Shear Stress Transport, SST) tends to predict an unphysical separation on upper surface of flap. By intensifying grid of fully turbulent cases, the relative error of lift and drag coefficients between simulation and experiment can be reduced by 0.8% and 1.5%. Meanwhile when incorporating transitional modeling without intensifying grid, the corresponding errors can be reduced by 4.01% and 5.1% , which can still be further reduced by grid intensification. The results and conclusions in this essay can be applied to the design of Natural Laminar Airfoil with high lift configurations.

1. Introduction

High-lift systems are crucial elements in design of commercial and civil airplanes. They significantly increase the lift of the aircraft at low speed during landing and take-off phases. The design of such configurations is challenging because the flow structure surrounding the shape is complex, which usually involves separation, shear layer, etc. Previous computational and experimental study is conducted to understand the flow physics related to high lift configurations, yet they were often forced turbulent in order to avoid the interruption of transition^[1].

This research focuses on the effect of transition on aerodynamic characteristics of high lift configurations. To investigate transitional effect, numerical simulations are conducted on multiple airfoil *McDonald Douglas 30P30N* and *NASA Trapezoidal Wing*. The simulations are accomplished by an in-house code, which is validated with the results of experiments on *Natural Laminar Airfoil*. The free transition is simulated with γ - $Re_{\theta t}$ transition model. To accelerate the convergence rate of the code, a multi-level multigrid methodology is adopted: The inviscid, laminar, turbulent and transitional flow simulations are conducted by multigrid method on grids of different grid density consecutively.

The calculated results for the typical high lift configurations are compared with experiments in NASA Langley low turbulent wind tunnel. Firstly, The cases predict the transition onset positions on main airfoil upper/lower surface and the flap upper surface successfully. Besides, to investigate the importance of transition in simulations, test cases are run with and without transitional modeling. The results show that using fully turbulent model (Shear Stress Transport, SST) tends to predict an unphysical separation on upper surface of flap, and increasing the grid density doesn't improve the situation. However, when incorporating transitional model in the simulation (SST+ γ - $Re_{\theta t}$), the flow is attached and the pressure and friction distribution is much closer to the experiment. The distribution of vortex and turbulent energy are analyzed to explain the difference. Furthermore, grid dependency is studied. By intensifying grid of fully turbulent cases, the relative error of lift and drag coefficients between simulation and experiment can be reduced by 0.8% and 1.5%. Meanwhile when incorporating transitional modeling without intensifying grid, the corresponding errors can be reduced by 4.01% and 5.1% , which can still be further reduced by grid intensification. The results and conclusions in this essay can be applied to the design of *Natural Laminar Airfoil* with high lift configurations.

2. Implementation of the transitional model

2.1 Framework of the γ - $\text{Re}_{\theta t}$ transitional model

Mentor's two-equation γ - $\text{Re}_{\theta t}$ transitional model is implemented in the in-house code for CFD simulation. The governing equations of γ - $\text{Re}_{\theta t}$ model are as follows:

$$\frac{\partial(\rho\gamma)}{\partial t} + \frac{\partial(\rho U_j \gamma)}{\partial x_j} = P_\gamma - E_\gamma + \frac{\partial}{\partial x_j} \left[\left(\mu + \frac{\mu_t}{\sigma_f} \right) \frac{\partial \gamma}{\partial x_j} \right] \quad (1)$$

$$\frac{\partial(\rho \overline{\text{Re}_{\theta t}})}{\partial t} + \frac{\partial(\rho U_j \overline{\text{Re}_{\theta t}})}{\partial x_j} = P_{\theta t} + \frac{\partial}{\partial x_j} \left[\sigma_{\theta t} (\mu + \mu_t) \frac{\partial \overline{\text{Re}_{\theta t}}}{\partial x_j} \right] \quad (2)$$

where γ is the intermittency and $\overline{\text{Re}_{\theta t}}$ is the transitional momentum thickness Reynolds number. In practical, the transitional model needs to be implemented in combination with a turbulent model in the RANS framework. In this essay, the Shear Stress Transport (SST) is the adopted turbulent model. The modified governing equations with respect to the SST- γ - $\text{Re}_{\theta t}$ model is as follows

$$\frac{\partial(rk)}{\partial t} + \frac{\partial(rU_j k)}{\partial x_j} = P_{k,\text{eff}} - E_{k,\text{eff}} + \frac{\partial}{\partial x_j} \left[\left(m + \frac{m_t}{S_k} \right) \frac{\partial k}{\partial x_j} \right] \quad (3)$$

$$\frac{\partial(\rho\omega)}{\partial t} + \frac{\partial(\rho U_j \omega)}{\partial x_j} = P_\omega - E_\omega + \frac{\partial}{\partial x_j} \left[\left(\mu + \frac{\mu_t}{\sigma_f} \right) \frac{\partial \omega}{\partial x_j} \right] + X_\omega \quad (4)$$

The transitional effect is reflected in the turbulent production term $P_{k,\text{eff}} = \gamma P_k$ and destruction term $E_{k,\text{eff}} = \min(\max(\mathcal{G}_{\text{eff}}, 0.1), 1) E_k$ in equation (3). The other definitions, terms and empirical coefficients related to equations(1)-(4) are available to the community [2] so they are not mentioned here.

2.2 Code implementation

The in-house CFD code based on finite volume method is used in the essay. The convection term of the Navier Stroke's equations is discretized by AUSMDV [3] scheme, and the diffusion term is discretized by central difference scheme. Time marching is established by implicit LU-SGS [4].

To accelerate the convergence rate and robustness of the code, a multi-level multigrid methodology is adopted as follows. By neglecting every other node in the calculation mesh, a coarser level of grid unit can be constructed by combining the adjacent eight grid units in the three dimensional space. The grid can be further coarsened by this approach as long as the number of nodes is adequate. Multigrid method can be conducted on the grid series to accelerate the convergent rate. To further enhance the robustness of the code, a multi-level multigrid method is adopted. In brief, the result of coarser grid is interpolated on a finer grid as the initial flow field for recalculation. To be more specific, first the inviscid flow is calculated for several steps on the coarsest level of grid by single grid because the grid cannot be further coarsened; then the result is interpolated on a finer level of grid as the initial flow field to continue laminar calculation, during which multigrid is adopted; after that the laminar flow is interpolated on a finer level of grid to continue turbulent flow calculation, when multigrid is adopted; finally, when fully turbulent flow reaches convergence, the transitional calculation starts to iterate.

2.3 Code verification

To validate the accuracy of the code, flow around natural laminar airfoil NLF0416 is simulated. The freestream condition is: $\text{Ma} = 0.1$, $\text{Re} = 2.0 \times 10^6$, angle of attack = 1° , turbulent intensity $\text{Tu} = 0.3\%$. The result of the simulation is compared with experiments from NASA Langley Low-Turbulence Pressure Tunnel (LTPT) [5].

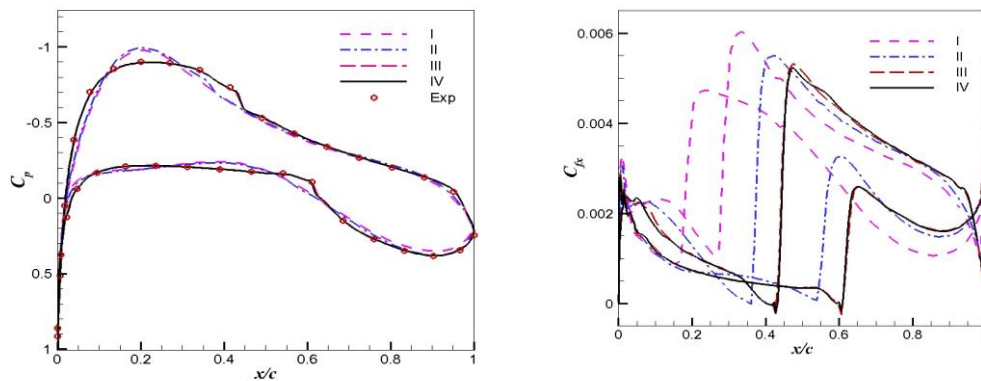
Four sets of grid with different number of cells are used to identify the impact of grid resolution on transition prediction, and the results are shown in Table 1. The first column is the circumferential cell number \times radial cell number. x_{tr}^u and x_{tr}^l denotes the location of transition onset on the upper and lower surface respectively. C_d and

C_l are the drag and lift coefficients. To satisfy the requirements of transition model^[2], the first layer of mesh is 10^{-5} m away from the solid wall to achieve $y^+ \leq 1.0$. The growth ratio in the direction normal to the wall is 1.1.

Table 1 Impact of grid resolution on simulation

Cases	x_{tr}^u/m	x_{tr}^l/m	C_d	C_l
I(164×68)	0.16	0.27	0.0089	0.44
II(232×96)	0.36	0.54	0.0065	0.47
III(329×136)	0.43	0.61	0.0056	0.54
IV(465×192)	0.43	0.61	0.0057	0.54
Experiment	0.4-0.45	0.6-0.65	0.0055	0.53

Fig.1 shows the pressure distribution. As an ordinary and convenient practice^[2], the onset of transition is recognized by a sharp increase in the frictional force curve. It can be observed that coarse grid (I, II) fails to reflect minor change in pressure coefficients distribution near transitional region and the onset is predicted poorly. In contrary, the intensified grid (III and IV) can predict the change of force coefficients near transition quite well. Therefore with accurate grid intensity, in-house CFD code with transitional model can predict the onset of transition well with the experiments.



a) The pressure coefficient b) The frictional coefficient in x dimension

Figure 1. Grid sensitivity for the CFD calculation

3. Numerical simulation of the three-element high lift airfoil

McDonald Douglas 30P30N is the benchmark case of the High-Lift CFD Workshop held in 1993 by NASA's Langley Research Center^[6]. Due to the drastic changes in pressure gradient and kinetic energy surrounding the geometry, the precise calculation is very challenging. Because it reflects the geometric characteristic and typical mechanism for high lifting, this 2-dimensional case is chosen to investigate the effect of transition on high lift configuration aerodynamics. The corresponding experiments were conducted in Langley's low turbulent wind tunnel and provide information on lift/drag coefficient^[6]. Hot film is used to detect transition onset on each element^[6]. The frictional coefficient is measured by Preston tube^[6]. The flow fields of the present geometry are simulated with an in-house code and are compared with the experimental results. The grid for calculation is shown in Fig.2. The distance of the first layer of grid satisfies $y^+ < 1$. To guarantee the accuracy of the frictional force, grids of different intensities are run until grid independency is achieved. For briefing, only the results corresponding to grid independency are shown here. The final grid quantity is 125 thousand. Grid in regions of the detached shear layer from main slat and main element is intensified to improve description of the mixture and vortex dominating flows.

The inflow parameters are given as follows:

$$\text{Ma} = 0.2, \text{Re} = 9 \times 10^6, \text{AoA} = 8^\circ, C_{\text{ref}} = 0.5588\text{m}$$

The comparison of the lift (C_l) and drag (C_d) coefficients between the calculations and experiments are shown in Table.2.

Table 2 Comparison of the lift/drag coefficient

	Experiments	SST calculation	SST+transition calculation
C_l	3.18	2.5257	2.7300
C_d	0.0276	0.0453	0.03894

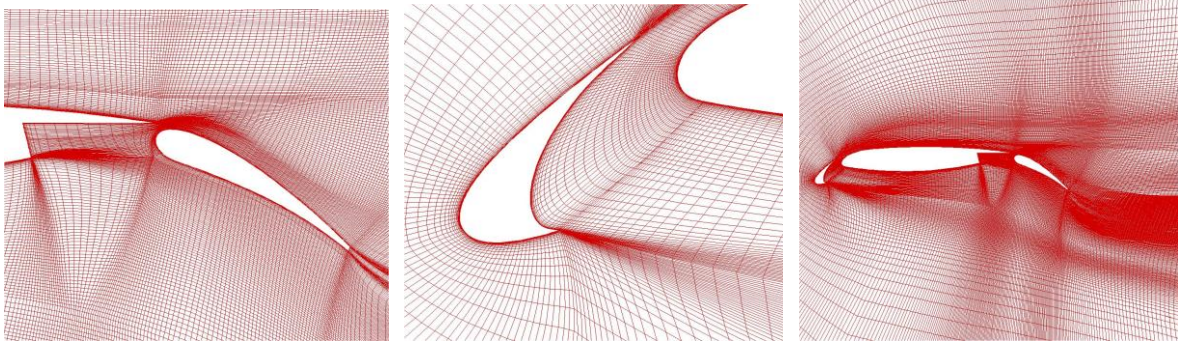
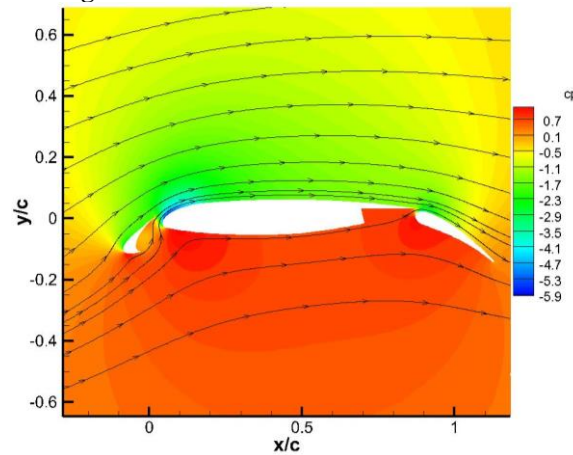
**Figure 2. Grid details for 30P30N test case****Figure 3. Pressure contour and streamline for 30P30N test case**

Fig.3 shows the contour of pressure coefficient and streamlines. It can be observed that flow passes through the gap between the slat and the main element and the gap between the main element and flap. At a relatively high angle of 8° , the flow leakage at the above mentioned positions relieves the adverse pressure gradient on the upper face, thereby suppress separation and delay stall. Meanwhile it can be observed that due to the high speed flow on upper face, the three negative pressure peaks are obvious, all contributing to high lift.

Fig.4 shows the comparison between the calculated and experimental pressure coefficient. It is worth mentioning that when only turbulent flow is considered, pressure plateau due to flow separation occurs in the rear region of the flap, which is inconsistent with the experiment. Yet when transitional model is adopted, the flow separation doesn't exist anymore. This is possibly caused by the more realistic distribution of the turbulent kinetic energy. Besides, the suction peak in the main element is better simulated when accounting transition.

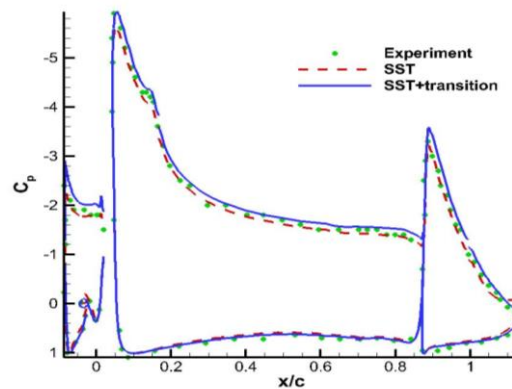
**Figure 4. Comparison for the pressure distribution**

Fig.5 is the comparison of the frictional coefficient distribution. When adopting γ - Re_{θ} model, transition regions are evident on both sides of the main element and upper flap. The typical trend is a rise from a lower level to what is close to the turbulent value, the position of which is then identified as the onset of transition as listed in Table.2. The predicted positions fit well with the experiment. Similar to the pressure distribution, the predicted frictional coefficients on the flap rear region coincide with the experiments.

Table 2 Comparison of the transition onset on all elements

$x_{tr,onset}$ (x/c)	Upper slat	Lower slat	Upper main	Lower main	Upper flap	Lower flap
Experiment	-0.057	-	0.057	0.526	0.931	-
CFD	-	-	0.085	0.539	0.920	-

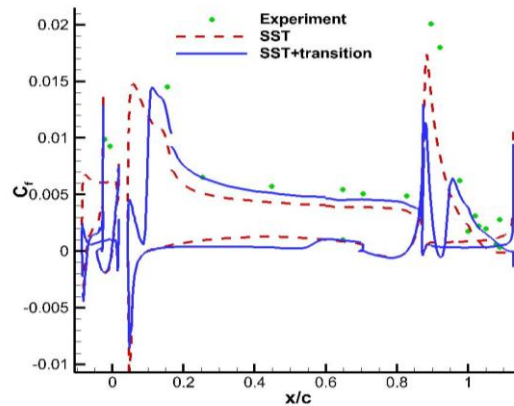


Figure 5. Comparison for the frictional coefficient distribution

Fig.6 shows the turbulent kinetic energy surrounding the three elements. The transition onsets on upper/lower main element and upper flap can be observed as a rise in kinetic turbulent energy in the boundary layer.

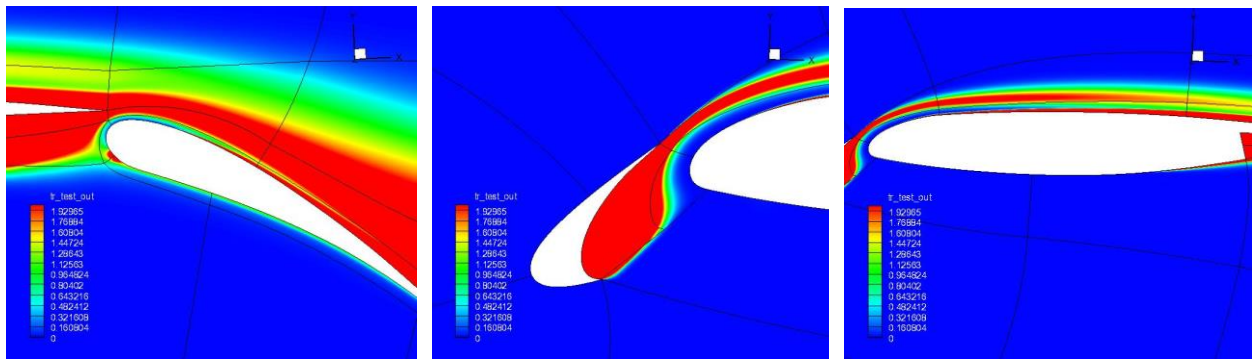


Figure 6. Contour of the turbulent kinetic energy

4. Numerical simulation of high lift configuration

So far we have analyzed the impact of transition on two-dimensional high lift configurations. To further verify the conclusions, a three-dimensional geometry is simulated in this chapter. The geometry is the NASA "Trapezoidal Wing" of the first high lift prediction workshop^[7], as shown in Fig.7. Its lift/drag, pressure distribution, and velocity profile are measured in NASA's Langley 14' \times 12' wind tunnel^[8]. The workshop provides two configurations with different deflection angles. In this essay, only Config1, of which slat angle is 30°, flap angle is 25° and without bracket is simulated according to the following freestream condition.

$Ma = 0.2$, $AoA = 13^\circ$, $Re = 4.3 \times 10^6$, $T_{ref} = 520R = 288.89K$, $S_{ref} = 22.028 \text{ ft}^2 = 3172.032 \text{ in}^2$.

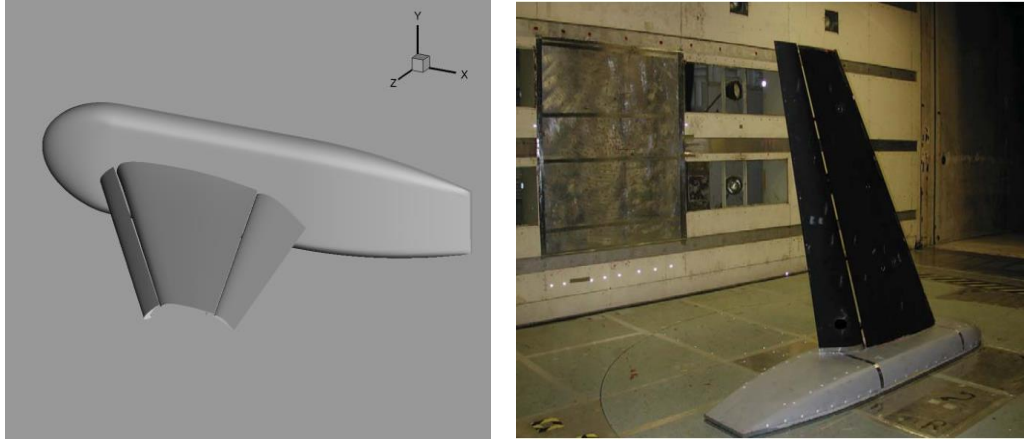


Figure 7. Geometry of the NASA "Trapezoidal Wing"

The lift/drag coefficients from the experiments are as follows:

$$C_l=2.047, \quad C_d=0.333203.$$

The structured grids provided by the workshop are used for the simulation, as described in Table.3. The requirement of $y^+ < 1$ is satisfied in all grids.

Table.3 Description of the grids and the calculated lift/drag coefficients

Case	Grid	Total cell/million	C_l	C_d	Description
(A)	Coarse	20	1.941	0.308	SST
(B)	Medium	48	1.959	0.313	SST
(C)	Coarse	20	2.0267	0.3247	SST+transition

4.1 Fully turbulent flow by the coarse grid

In this section, the results on spanwise locations i.e. $y_{ita}=50\%$, 85% and upper flap are compared and analysed. It can be observed from Fig.8 that by using coarse grid and SST turbulent model, the pressure distribution on rear flap is poorly simulated. Similar to the 30P30N case, an unphysical separation is evident in the rear flap. Meanwhile, it can also be observed that relative large discrepancy occurs in the front part of the flap and rear part of the main element. This illustrates that the flow inside the channel (concave) region is not calculated properly. This argument can be further strengthened in Fig.8(c). The flow structure here includes the high speed flow in the concave region between slat and main element and the shear layer detached from the main element. Vortexes are assumed to be incorporated in the region. In summary, only using SST turbulent model and coarse grid cannot obtain convincing results.

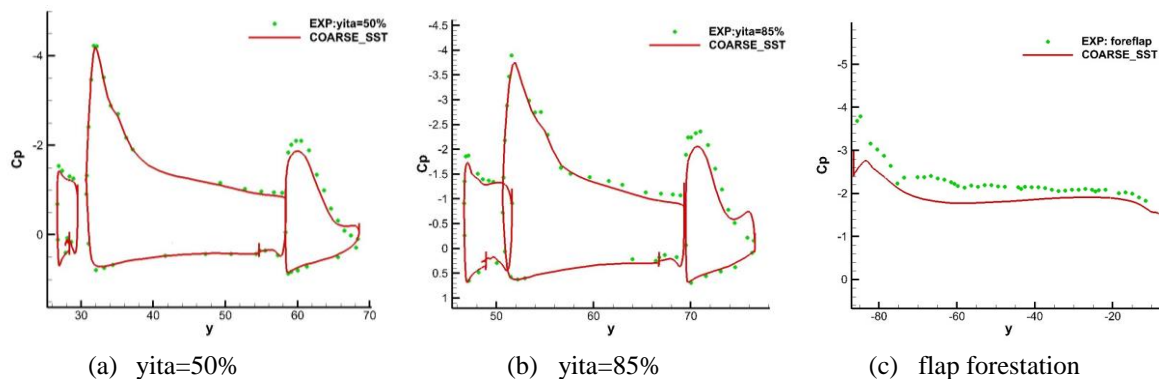


Figure 8. Pressure distribution comparison

Fig.9 shows the surface streamline when SST is adopted. It is evident that the separation occurs in the rear of the flap.

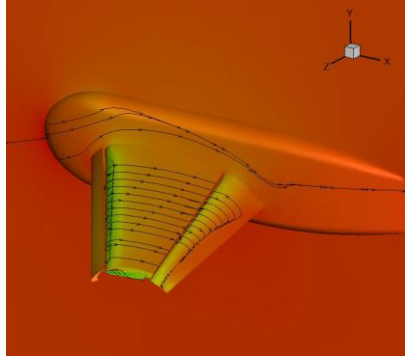


Figure 9. Surface streamline when flow is fully turbulent

4.2 Fully turbulent flow by the medium grid

The comparison of pressure coefficient are shown in Fig.10. It can be observed that by intensifying the grid, simulation goes towards the right trend. The improvement in $y_{ita}=50\%$ is not so obvious as $y_{ita}=85\%$. The pressure in the front part of the flap is higher while the pressure in the rear flap is lower, all showing a better fit towards experiment. This indicates that the description of the flow related to main element and flap is better simulated by a intensified grid. Yet the unphysical separation region is still obvious, indicating the inherent problem of using full turbulent model. If the calculated lift/drag coefficients as shown in Table.3 are compared with the experiments, it is shown that by intensifying grid of fully turbulent cases, the relative error of lift and drag coefficients between simulation and experiment can be reduced by 0.8% and 1.5%.

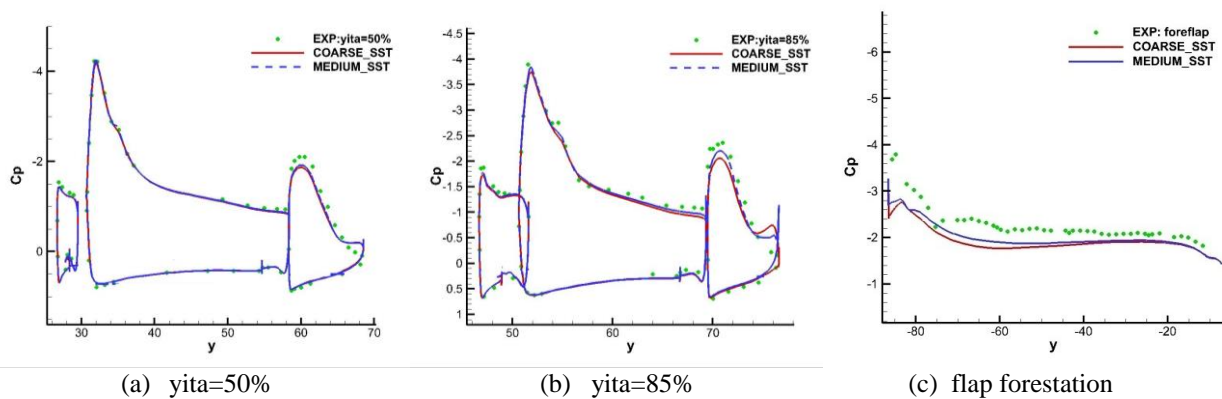


Figure 10. Pressure distribution comparison

4.3 Transitional flow by the coarse grid

As shown in Fig.11, when taking transition into consideration, a better capture of the flow physics is achieved without the necessity to further intensify the grid. To be more specific, the case in this section shows clear fit on the pressure distribution of slat and main element. Besides, in the rear flap region, the flow is attached which is consistent with the experiments and the pressure coefficient is almost the same as the experiments. From the view of lift/drag coefficient, intensifying the grid and including transitional effect both contributes to the better description of the flow feature. To be more specific, when incorporating transitional modeling without intensifying grid, the corresponding errors can be reduced by 4.01% and 5.1%, which can still be further reduced by grid intensification.

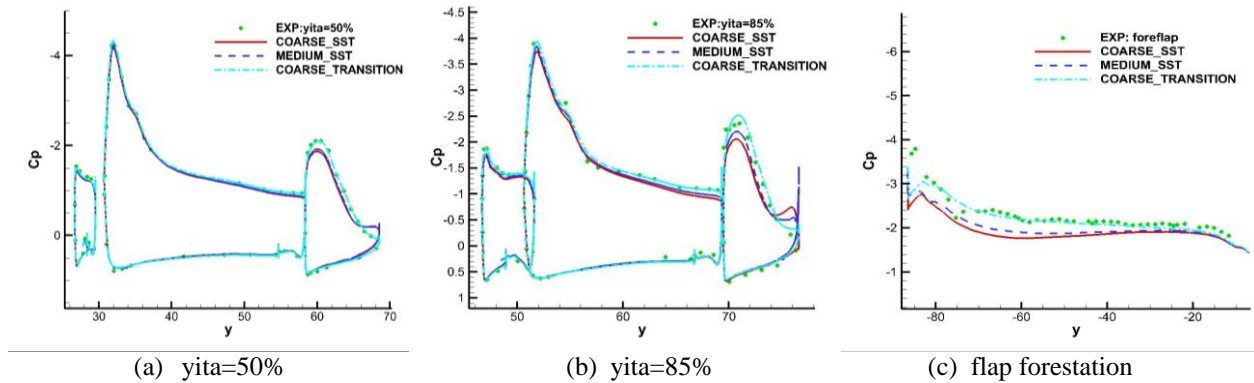


Figure 11. Pressure distribution comparison

5 Conclusions

In this essay aerodynamics related to typical high lift geometry is investigated. Influencing factors such as grid density, turbulent and transitional model are analysed. The following conclusions can be drawn:

1. When using SST turbulent model to simulate the high lift configurations, the pressure on slat and main element can be described correctly, but a unphysical separation occurs in the rear flap. Meanwhile the full turbulent frictional distribution deviates from the experiment results.
2. When transition model is included, the unphysical separation on rear flap doesn't exist any more, resulting in a better coincidence between simulation and experiment.
3. Further intensifying the grid can improve the lift and drag coefficient in the right trend. But such improvement is not so strong as considering transition model, which implies that transition affect the wall-bounded properties greatly. Only when taking into consideration of transition, the relevant physical quantities can be precisely captured.

References

- [1] Rumsey, C.L., Gatski, T.B., Ying, S.X. and Bertelrud, A., 1998, Prediction of High-Lift Flows Using Turbulent Closure Models, *AIAA Journal*, Vol. 36, No. 5.
- [2] Langtry, Robin B., and Florian R. Menter, Correlation-based Transition Modeling for Unstructured Parallelized Computational Fluid Dynamics Codes, *AIAA journal*, Vol.47, No.12, 2009, pp. 2894-2906.
- [3] Liou, M. S., and Y. Wada, A Flux Splitting Scheme with High-Resolution and Robustness for Discontinuities, *AIAA paper*, 1994, pp. 94-0083.
- [4] Chen, R. F., and Z. J. Wang, Fast, Block Lower-Upper Symmetric Gauss-Seidel Scheme for Arbitrary Grids, *AIAA journal*, Vol.38, No.12, pp. 2238-2245.
- [5] Somers, Dan M, Design and Experimental Results for a Natural-Laminar-Flow Airfoil for General Aviation Applications, *NASA Technical Paper* 1861, 1981.
- [6] Klausmeyer, S.M. and Lin, J.C., 1997, Comparative Results From a CFD Challenge Over a 2D Three-Element High-Lift Airfoil, *NASA Technical Memorandum* 112858.
- [7] L. Rumsey C, P. Slotnick J, Long M, et al. Summary of the First AIAA CFD High-Lift Prediction Workshop. *Journal of Aircraft*, 2011, (6):2068-2079.
- [8] Johnson, P. L., Jones, K. M., and Madson, M. D., Experimental Investigation of a Simplified 3D High Lift Configuration in Support of CFD Validation, *AIAA Paper 2000-4217*, August 2000